



LAWRENCE
LIVERMORE
NATIONAL
LABORATORY

Distinguishing Monosaccharide Stereo- and Structural Isomers with ToF-SIMS and Multivariate Statistical Analysis

E. S. F. Berman, K. S. Kulp, M. G. Knize, L. Wu,
E. J. Nelson, D. O. Nelson, K. J. Wu

May 5, 2006

Analytical Chemistry

Disclaimer

This document was prepared as an account of work sponsored by an agency of the United States Government. Neither the United States Government nor the University of California nor any of their employees, makes any warranty, express or implied, or assumes any legal liability or responsibility for the accuracy, completeness, or usefulness of any information, apparatus, product, or process disclosed, or represents that its use would not infringe privately owned rights. Reference herein to any specific commercial product, process, or service by trade name, trademark, manufacturer, or otherwise, does not necessarily constitute or imply its endorsement, recommendation, or favoring by the United States Government or the University of California. The views and opinions of authors expressed herein do not necessarily state or reflect those of the United States Government or the University of California, and shall not be used for advertising or product endorsement purposes.

Distinguishing Monosaccharide Stereo- and Structural Isomers with ToF-SIMS and Multivariate Statistical Analysis

Elena S.F. Berman^{1}, Kristen S. Kulp¹, Mark G. Knize¹, Ligang Wu², Erik J. Nelson², David O. Nelson³,
Kuang Jen Wu²*

AUTHOR ADDRESS ¹Biosciences Directorate, ²Chemistry and Materials Science Directorate, and ³Computation Directorate, Lawrence Livermore National Laboratory, 7000 East Avenue, Livermore, CA 94550

AUTHOR EMAIL ADDRESS berman2@llnl.gov

RECEIVED DATE (to be automatically inserted after your manuscript is accepted if required according to the journal that you are submitting your paper to)

TITLE RUNNING HEAD. Distinguishing Monosaccharide Isomers with ToF-SIMS

CORRESPONDING AUTHOR FOOTNOTE. *Biosciences Directorate, Lawrence Livermore National Laboratory, 7000 East Avenue L-446, Livermore, CA 94550 berman2@llnl.gov

ABSTRACT. Time-of-Flight Secondary Ion Mass Spectrometry (ToF-SIMS) is utilized to examine the mass spectra and fragmentation patterns of seven isomeric monosaccharides. Multivariate statistical analysis techniques, including principal component analysis (PCA), allow discrimination of the extremely similar mass spectra of stereoisomers. Furthermore, PCA identifies those fragment peaks which vary significantly between spectra. Heavy isotope studies confirm that these peaks are indeed sugar fragments, allow identification of the fragments, and provide clues to the fragmentation pathways.

Excellent reproducibility is shown by multiple experiments performed over time and on separate samples. This study demonstrates the combined selectivity and discrimination power of ToF-SIMS and PCA, and suggests new applications of the technique including differentiation of subtle chemical changes in biological samples that may provide insights into cellular processes, disease progress, and disease diagnosis.

KEYWORDS (Word Style “BG_Keywords”). Mass Spectrometry, ToF-SIMS, glucose, fructose, monosaccharides, PCA

MANUSCRIPT TEXT (Word Style “TA_Main_Text”).

Introduction

Time-of-Flight Secondary Ion Mass Spectrometry (ToF-SIMS) is a soft-ionization, surface-sensitive mass-spectral technique which has recently demonstrated applications in the analysis of biomaterials and biological samples.^{1, 2} ToF-SIMS measurements use a finely focused (~200 nm) energetic primary ion beam to desorb secondary molecular and fragment ions into a time-of-flight mass spectrometer. Desorption and ionization are simultaneous, allowing investigation of compounds which readily degrade or are difficult to ionize, such as underivatized monosaccharides. Coupling the SIMS ionization with a time-of-flight mass spectrometer permits fast analyses over a wide mass range with good mass resolution (~7000 at $m/z = 41$).

ToF-SIMS is routinely used to identify the chemical and molecular composition of a surface. Since a ToF-SIMS spectrum often contains peaks representing the molecular ions or large fragments of the parent compounds in the sample, these compounds can be identified or confirmed by careful analysis of characteristic peaks in the ToF-SIMS spectra. Furthermore, small variations in the samples can be detected by differences in the fragmentation pattern in the mass spectra. This has proven to be

extremely useful for ascertaining minute variations in side chains or end groups of synthetic polymers with nearly identical backbone repeat structures.

The analysis of biological samples presents unique challenges to ToF-SIMS. Biological samples are at the same time enormously complex and quite similar to one another. Additionally, important components are often represented at extremely low concentrations. For efficient analysis of biological samples, sufficient sensitivity is needed to detect low abundance components and sufficient selectivity is required to discriminate between the very similar molecules and closely related samples. In this study we demonstrate the extraordinary selectivity of ToF-SIMS analysis by distinguishing between stereo- and structural isomers of biologically relevant monosaccharides.

Complex biological environments also produce complex mass spectra which are difficult if not impossible to interpret in conventional ways. Multivariate statistical analysis and pattern recognition techniques are widely employed for interpretation of such complex data sets, as they reduce the data complexity and illuminate distinguishing features from the data. In this work, Principal Component Analysis (PCA) has been used to identify similarities and differences in ToF-SIMS spectra and classify spectra into groups.³ PCA, a standard, unsupervised multivariate statistical technique, reduces a large data matrix to a few manageable variables that can be visualized and interpreted using a series of simple plots. PCA reduces the data complexity by calculating new variables called principal components, which represent linear combinations of the original variables and capture the greatest variation in the data set. The molecular fragments with the highest variance in intensity among the statistical groups identify important differences between samples. Wagner and Castner have used PCA to successfully cluster ToF-SIMS mass spectra generated from samples of single proteins.⁴

A particular challenge for mass spectrometry techniques is distinguishing and characterizing isomers. With identical elemental composition, and thus the same molecular weights, isomers exhibit the same molecular ion peak and share the same fragment ions in the mass spectra. Although generally considered indistinguishable by conventional spectral interpretation, we show that isomers can be

distinguished by analyzing the overall spectral pattern in which each isomer displays its unique relative abundance of fragment ions.

For this work, simple monosaccharides were chosen for analysis due to their biological significance, relative abundance in biological samples, and complex array of similar structures. Monosaccharides are the basic building blocks of all carbohydrates, the central metabolic currency of life. In addition, monosaccharides are principal constituents of nucleic acids and important elements of lipids and proteins. Glycoproteins, proteins covalently linked with carbohydrates, are essential in intracellular communication, the formation of bacterial cell walls, and, when arrayed on the cell surface, comprise unique cellular markers. In fact, saccharides are the most abundant group of biomolecules and are essential to all living organisms.⁵ Clearly, the detection of monosaccharides and their derivatives will be an important aspect of analysis and characterization of any biological sample.

Due to their critical position in biology, much mass spectral analysis has been focused on carbohydrates. Early work includes several studies of derivatized monosaccharides by Biemann et al.,⁶ DeJongh et al.⁸⁻¹⁰ and Caprioli et al.¹¹ These researchers found that underivatized monosaccharides were insufficiently volatile and extremely sensitive to heat, rendering them unsuitable for conventional electron impact mass spectrometry. However, by derivatizing the sugars, they were able to distinguish between structural isomers, although stereoisomers produced indistinguishable spectra. Early work on derivatized sugars has been reviewed by Lonngren and Svensson.¹² Analysis of simple sugars has continued with field desorption mass spectrometry,¹³ liquid-assisted secondary ion mass spectrometry,¹⁴ quadrupole time-of-flight tandem mass spectrometry,¹⁵ and inductively coupled plasma and electrospray ionization.¹⁶ Zapfe et al.¹⁴ and March et al.¹⁵ were able to distinguish stereoisomeric hexoses with the use of post-ionization fragmentation and tandem mass spectrometry on selected sugar fragments. Vink et al.¹⁷ were able to identify stereoisomers of derivatized sugars utilizing peak selection and ratio comparison. In this work underivatized isomers are distinguished in a single mass spectrometric stage with minimal data analysis time.

Significant research has also focused on the analysis of disaccharides and oligosaccharides, especially focused on determining the structures of linkages between monosaccharides. Infrared laser desorption/ionization,¹⁸ tandem mass spectrometry,¹⁹ post-source decay in matrix-assisted laser desorption ionization mass spectrometry (MALDI-MS)²⁰ and multicollision dissociation threshold analysis²¹ have all been utilized with some success. None of these techniques, however, has been used to fully differentiate between monosaccharide isomers.

Experimental Section

Monosaccharides.

Galactose, glucose, fructose, mannose, psicose, sorbose, and tagatose were obtained from Sigma (St.Louis, MO) and used without further purification. D-Glucose-U-¹³C₆ was obtained from Cambridge Isotope Laboratories (Andover, MA) and used without further purification. Each sugar was diluted in Milli-Q purified water (Millipore, Billerica, MA) to an approximate concentration of 1 mg/ml, after which 1µl was spotted on a silicon (Si) wafer and allowed to evaporate at room temperature. All seven sugars and the ¹³C glucose were spotted on each 0.5 × 0.5 inch wafer. A clean silicon wafer was placed on top of the dry sample substrate and pressed to 100 psi momentarily to flatten the sugar spots for improved ToF-SIMS analysis.

ToF-SIMS Analysis.

ToF-SIMS measurements were conducted on a PHI-TRIFT III instrument (Physical Electronics USA, Eden Prairie, MN) equipped with a gold (¹⁹⁷Au) liquid metal ion gun utilizing Au⁺ ions, operated at 22kV and in bunched-ion mode. Positive ion ToF-SIMS spectra were acquired over an area of 100 x 100 µm; three to ten spectra were recorded for each sugar spot. The samples were held at room temperature before and during the course of the ToF-SIMS measurements. All ToF-SIMS spectra were

calibrated to the CH_3^+ , C_2H_3^+ , and C_4H_7^+ peaks before analysis. Identical experiments were performed over a period of two months to monitor variation in and generalizability of the results.

Statistical Analysis.

In an effort to establish reproducibility, we have applied the following data preprocessing: for each mass spectrum, peaks due to sodium, potassium and silicon were removed after which the spectrum was normalized to the total ion count of the remaining peaks.

The between-substrate standard deviation and the within-substrate standard deviation for a given m/z peak was estimated by means of a linear mixed-effect model.²² The model used was the standard one for a blocked one-way layout, containing a fixed effect for the sugars and two nested random effects: one for sample substrates, and one for the residual deviation within any given substrate. The average ratio of the between-substrate to within-substrate standard deviations was estimated by regressing the logarithm of the between-substrate standard deviations on the logarithm of the within-substrate standard deviations. A simple linear representation was used (slope and intercept) to model the relationship, and a robust fitting method was employed to discount the effect of any single potential outlier. The slope parameter was not significantly different from one, indicating that the ratio was not detectably different across the range of values for the residual standard deviation. The ratio was then calculated by taking the antilogarithm of the intercept parameter.

Data reduction of the complete data set was accomplished by mean-centering the data matrix of spectra and reducing the data set by principal component analysis (PCA) using MATLAB software v. 7.0 (MathWorks Inc., Natick, MA) along with PLS Toolbox v. 3.5 (Eigenvector Research, Manson, WA). The PCA software generates a scores plot for visualization of data relationships and a loadings plot for identification of important mass fragments. Ninety-five percent data contours were drawn using the `error_ellipse.m` code by J. Andrew Johnson of Binghamton University, acquired from the MATLAB Central File Exchange.

To determine the expected prediction error associated with a new, unclassified sample, a simple variable selection and expected prediction error analysis was applied to the complete set of experimental data. PCA was done on a portion of the data, the training set, after which the reduced data was used in a linear discriminant analysis to produce a classifier. The remaining data, the test set, was then reduced and classified based on this classifier. The predicted classes were compared to the actual classes for the test set, resulting in a count of the misclassified test cases. Finally, the prediction error was estimated by summing up the misclassified test cases and dividing by the size of the overall data set.

Results

Averages of ten representative mass spectra of each of the four furanose sugars, fructose, psicose, sorbose and tagatose are displayed in Figure 1. Intact molecular ion peaks were not observed in the positive ion ToF-SIMS spectra, however the spectra do show many characteristic monosaccharide fragments. The mass spectra are highly similar, as would be expected for stereoisomers. Only psicose, with the presence of a large potassium peak at $m/z = 39$ and the corresponding $[M+K]^+$ peak at $m/z = 219$, is visually distinguishable. A possible explanation for this observation will be discussed below. Averages of ten representative mass spectra of each of the three pyranose sugars, galactose, mannose, and glucose, as well as the heavy isotope ^{13}C glucose are displayed in Figure 2. Once again, the stereoisomers give nearly identical spectra which are also very similar to those of their structural isomers the furanoses.

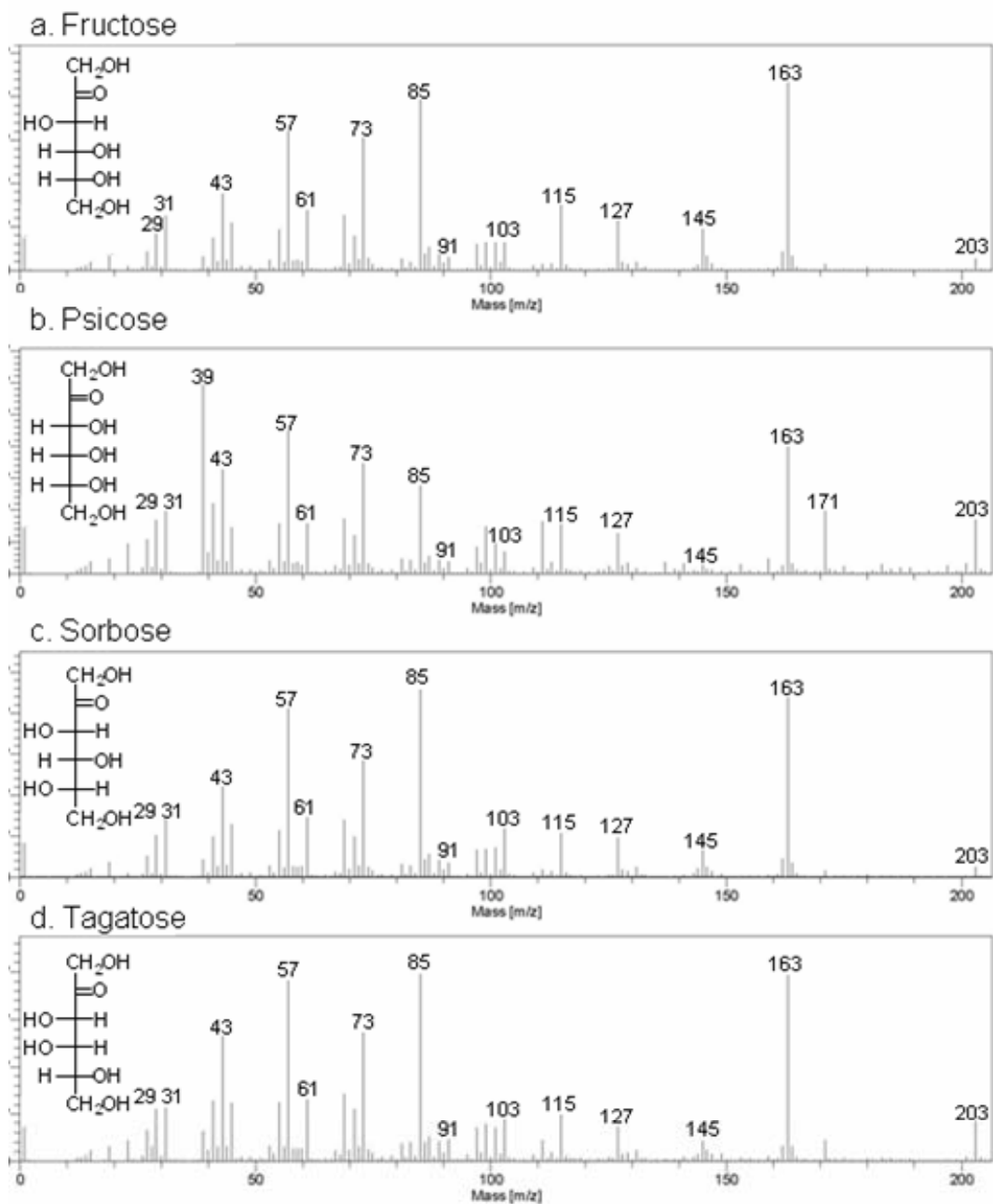


Figure 1: Average mass spectra of furanose monosaccharides: (a) fructose (b) psicose (c) sorbose and (d) tagatose.

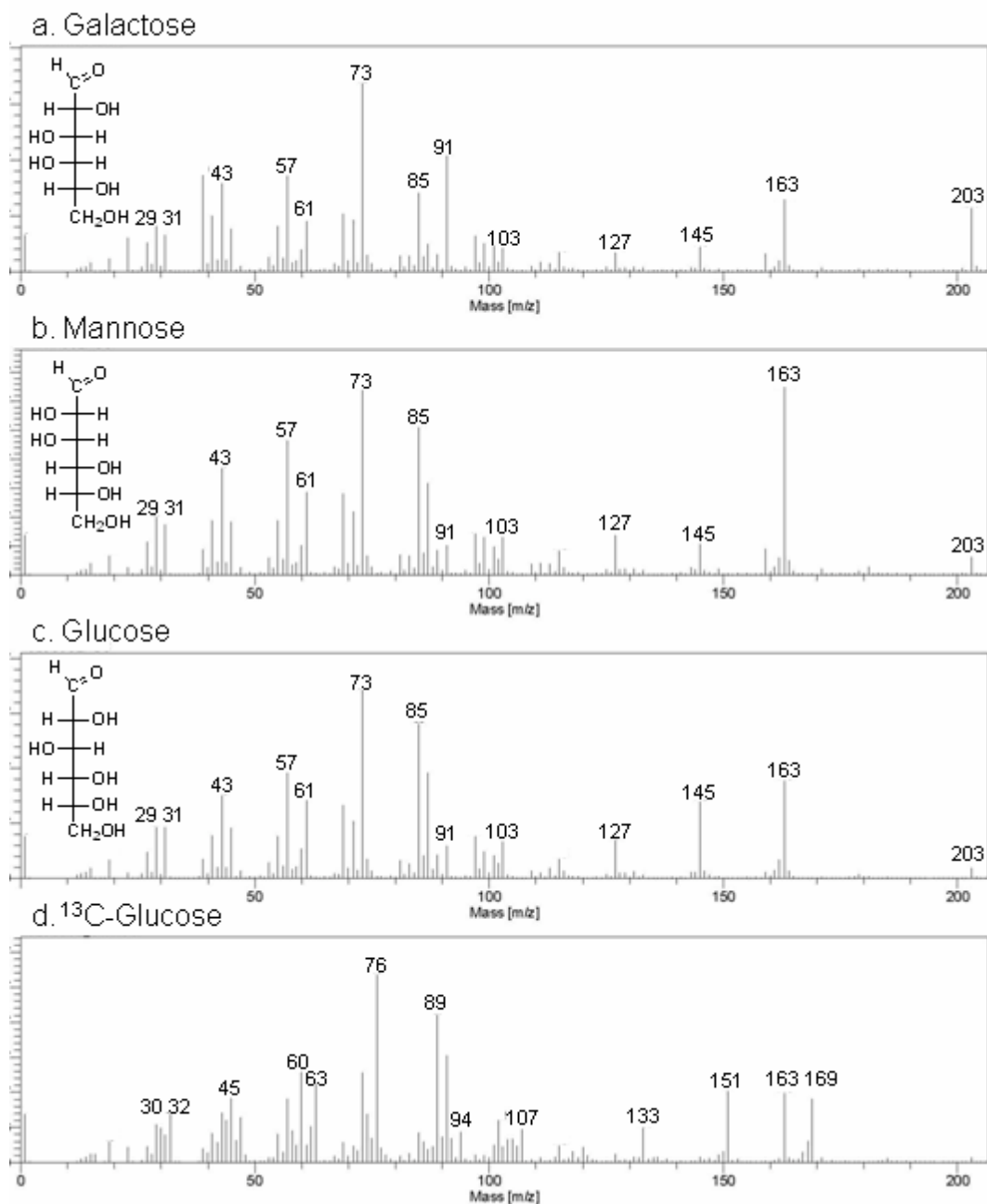


Figure 2: Average mass spectra of pyranose monosaccharides: (a) galactose (b) mannose (c) glucose and (d) D-glucose- $U\text{-}^{13}\text{C}_6$.

Due to the great similarity between the mass spectra of these isomeric sugars, differentiation by conventional methods appears impossible. Principal component analysis, however, is readily able to differentiate all seven isomeric hexoses. The PCA scores plot shown in Figure 3a illustrates the excellent clustering of mass spectra of individual sugars and separation of mass spectra from different sugars. The clustered spots are enclosed by ninety-five percent data contours. The loadings plot, Figure

3b, provides information as to which mass peaks are important in driving the achieved classification. Nearly all of the masses which are critical to the classification are identified as important sugar fragments.

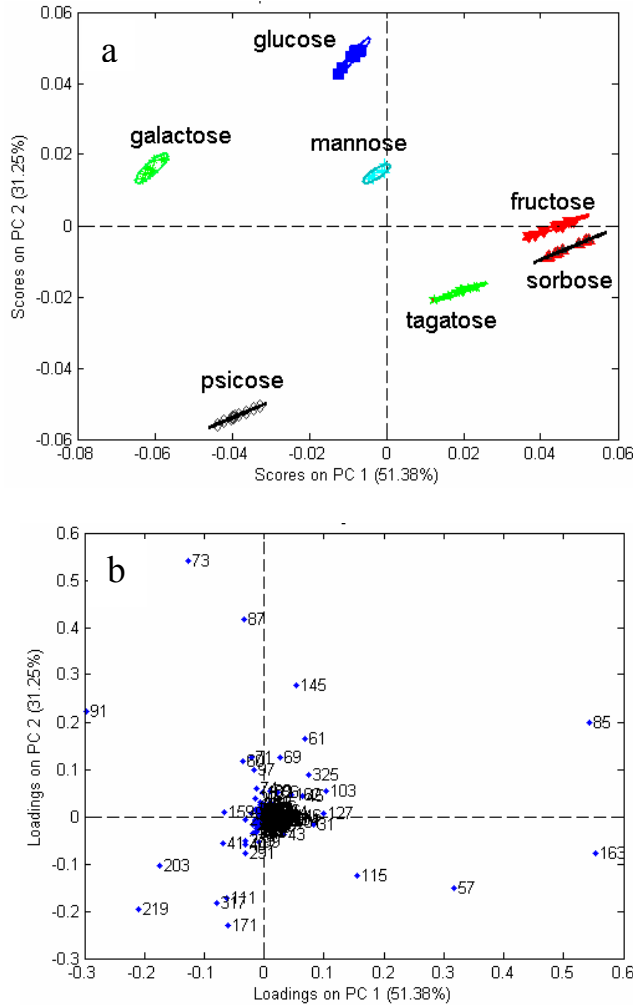


Figure 3: Scores plot (a) from principal component analysis data reduction of ToF-SIMS spectra from seven isomeric monosaccharides spotted on a silicon substrate. Data points are multiple analyzed areas from a single spot. Ellipses are 95% data contours. Loadings plot (b) showing masses responsible for discrimination between monosaccharides.

Figure 4 demonstrates the reproducibility of the combined ToF-SIMS/PCA technique. PCA has been performed on spectra taken from all seven sugars that were spotted on six separate silicon sample

substrates. These data were taken two months after those displayed in Figure 3a. As expected, there is some scatter from substrate to substrate, and some cluster of data from a given substrate. Overall, the excellent differentiation between stereoisomers remains evident and the similarity of the analyses is obvious.

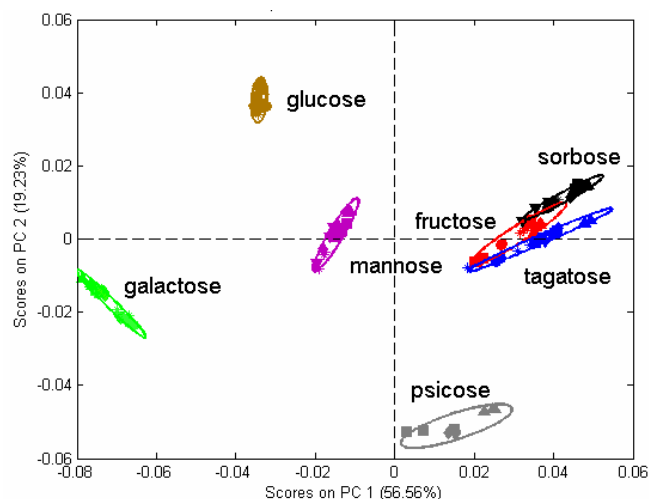


Figure 4: Scores plot from principal component analysis data reduction of ToF-SIMS spectra from six substrates each spotted with seven isomeric monosaccharides. The seven sugars are represented by the color scheme while the six substrates are represented by different shaped symbols: 1, ▼; 2, *; 3, ■; 4, ●; 5, ◆; 6, ▲. These data were taken two months after that shown in Figure 3a. Ellipses are 95% data contours.

Although the first two principal components are sufficient to differentiate an individual data set, the noise in the data causes the actual values of the loadings to differ from set to set. Hence, classifying new data using a classifier based on previous data may cause the new data to be classified incorrectly. To quantify the effect of noise like that observed in Figure 4 on discriminating sugars, we estimated the expected prediction error obtained by classifying a random future spectrum using the PCA-based classifier generated from the data displayed in Figure 3a. The classifier was generated as described in the statistical methods section above; Figure 5 shows the results of that analysis. We see that, in general, four or five principal components from one data set should be sufficient to classify future data with a

very high degree of accuracy. Given the large number of peaks contained in the mass spectra, this is a very significant reduction in the dimensionality of the data needed for classification.

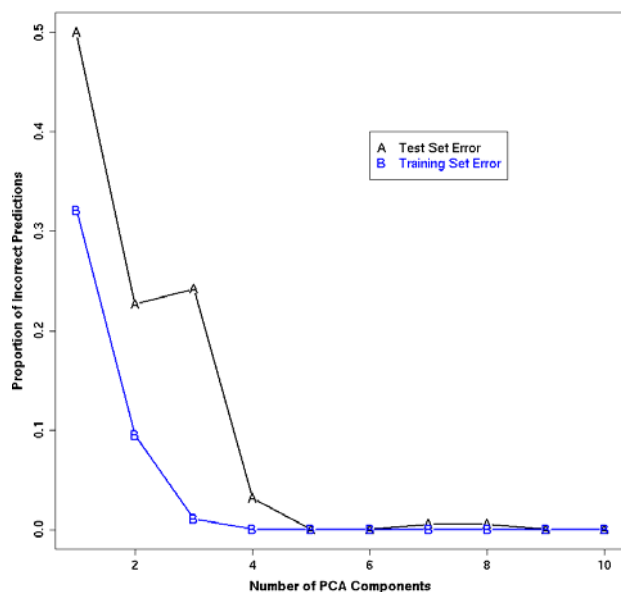


Figure 5: Expected prediction error as a function of the number of principal components used to classify future sugar spectra by linear discriminant analysis.

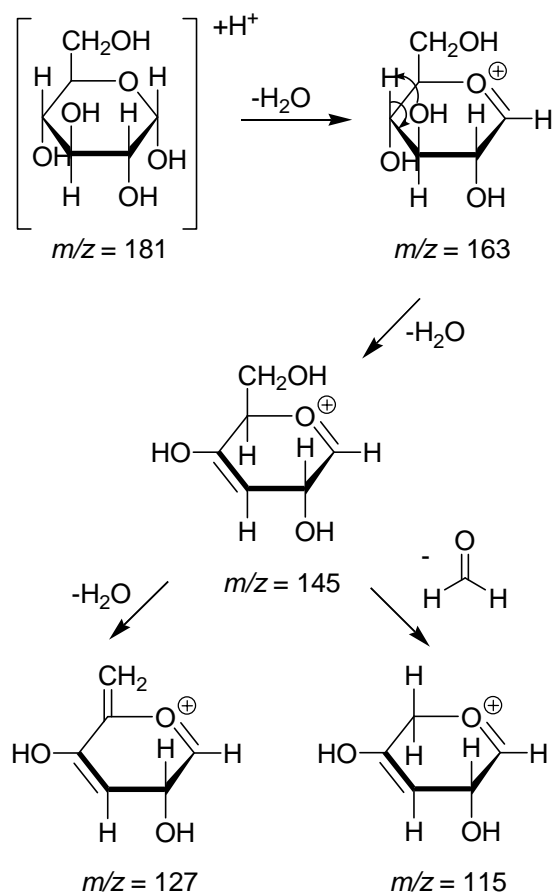
Discussion

In addition to the differentiation and classification of sugars made possible by this analysis, we have utilized the mass spectra to gain a better understanding of the fragmentation of these underivatized monosaccharides. The mass spectrum of glucose, Figure 2c, is considered in detail as a typical representative of the monosaccharides. Peak shifts between the glucose (Figure 2c) and ^{13}C glucose (Figure 2d) spectra are used to support fragment analyses and peak assignments. Fragmentation of fructose, galactose, mannose, psicose, sorbose and tagatose closely follows that of glucose with only minor modifications.

A very important mode of fragmentation for the monosaccharides is the successive loss of water from the alcohol functional groups. Scheme 1, adapted from Biemann et al. Scheme A,⁷ illustrates the successive loss of three water molecules from the protonated molecular ion, producing the ion series $m/z = 163, 145, \text{ and } 127$. The shifts of these peaks to $m/z = 169, 151, \text{ and } 133$ in the ^{13}C glucose spectrum

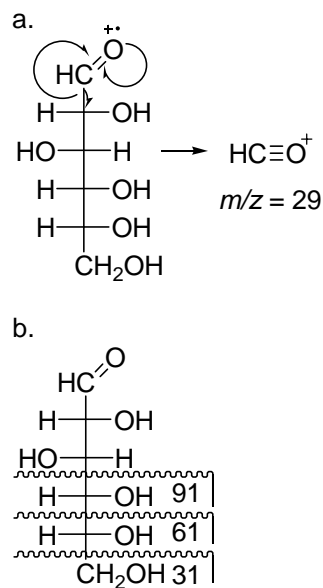
supports these fragment assignments, as do the exact molecular masses obtained from the high-mass-resolution ToF-SIMS. The apparent incomplete shift of peak $m/z = 163$ to 169 appears, by differences in cracking patterns and a lack of any other incomplete shifting, to be an impurity in the ^{13}C glucose. Scheme 1 also illustrates an additional proposed fragmentation by loss of the small neutral molecule formaldehyde. This loss results in the fragment of $m/z = 115$ which is more prominent in the furanose spectra than those of the pyranoses. This observation can be understood given the two locations for formaldehyde elimination, CH_2OH substituents, in the furanose sugars as opposed to one in the pyranoses. The assignment of the peak at $m/z = 115$ is supported by the closest molecular formula of $\text{C}_5\text{H}_7\text{O}_3$ to the high-resolution mass, by the appearance of a peak at $m/z = 120$ in the ^{13}C glucose spectrum and by the ICP analysis of Taylor et al.¹⁶

Scheme 1: Successive loss of water and/or formaldehyde from glucose.



Another important mode of fragmentation is that of α -cleavage as described by McLafferty and Tureček, p. 57.²³ Scheme 2 shows fragments formed by cleavage alpha to either unsaturated (a) or saturated (b) heteroatoms. These reactions account for peaks of $m/z = 29, 31, 61$ and 91 . Analysis of the ^{13}C glucose spectrum supports these fragment assignments with peaks shifting to $m/z = 30, 32, 63$ and 94 . High-resolution masses also support these assignments. The α -cleavage reaction would also be expected to result in a fragment of mass 121, but this peak is not observed to be significant in any of the sugar spectra.

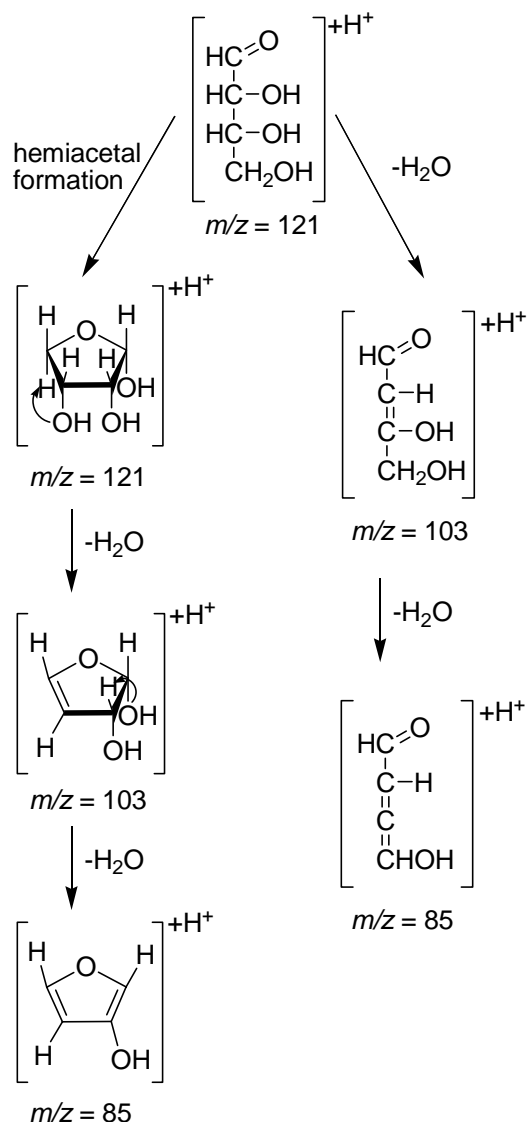
Scheme 2: Cleavage of glucose alpha to an unsaturated (a) or saturated (b) heteroatom.



Consideration of why the peak at $m/z = 121$ is not observed has led to the postulated fragmentation pathway illustrated in Scheme 3. The α -cleavage fragment of mass 121 is simply the protonated, four-carbon sugar D-erythrose. This sugar would be capable of forming the hemiacetal form, D-erythrofuranose as illustrated in the first step to the left on Scheme 3. Subsequent loss of water molecules, as in Scheme 1, produce fragments of $m/z = 103$ and 85 . These proposed fragmentations are corroborated by the most probable elemental compositions from high resolution spectra, $\text{C}_4\text{H}_7\text{O}_3$ and $\text{C}_4\text{H}_5\text{O}_2$ respectively. These assignments are further supported by the peak shifts from $m/z = 85$ to 89 and $m/z = 103$ to 107 in the ^{13}C glucose spectrum. The high intensity of the $m/z = 85$ ion bolsters this proposed structure as well, as the hydroxyfuran fragment is expected to be especially stable due to

aromaticity. It is also possible that the loss of water occurs without the cyclization, producing the fragments illustrated in the right fork of Scheme 3. However, the ICP analysis of Taylor et al.¹⁶ supports the ring structures for these fragments.

Scheme 3: Loss of water after α -cleavage of glucose to produce fragments of $m/z = 103$ and 85.



The base peak for many of the pyranoses at $m/z = 73$ has been identified by Biemann et al.⁷ as $\text{HO}-\text{C}^+-\text{OH}$, and a mechanism for its formation has been proposed by Lonngren and Svensson.¹² Our work supports this assignment both by high mass resolution ($\text{C}_3\text{H}_5\text{O}_2$) and the shift of this peak from $m/z = 73$ to 76 in the ^{13}C glucose spectrum. DeJongh's¹⁰ assignment of $m/z = 57$ to $\text{HO}-\text{C}^+-\text{CH}_2$ and Biemann's⁷ assignment of $m/z = 43$ to CH_3CO^+ are similarly confirmed. Alkali metal cationization of

monosaccharides is well known,^{19, 21, 24} suggesting that the relatively small peak at $m/z = 203$ is due to the $[M+Na]^+$ adduct and the similar $m/z = 219$ peak most evident in the psicose spectrum is due to the $[M+K]^+$ adduct.

Of the significant peaks in the mass spectra, only one is unassigned by this analysis. The rather large peak at $m/z = 87$ is determined by high resolution to be of molecular formula $C_4H_7O_2$; the shift of this peak to $m/z = 91$ in the ^{13}C glucose spectrum supports this conclusion. However, the reactions which lead to this fragment are unknown at this time.

Given the similarity of both the mass spectra and the fragmentation patterns of these stereo- and structural isomers, it is remarkable that PCA of the mass spectral data (Figure 3) reveals consistent grouping of spectra from the same sugar and separation of different sugars. Inspection of the loading plot, Figure 3b, shows that the differentiation of sugars is indeed due to sugar fragments rather than sample impurities or other confounding peaks. Furthermore, one can see that the pyranoses, glucose, galactose and mannose, tend to favor fragmentation into sections with masses 73, 87, and 91 while the furanoses, fructose, psicose, sorbose and tagatose, tend to fragment into masses 57, 85, 115, and 163. In addition, psicose shows a relatively large contribution from the alkali metal adducts of the molecular ion. It is postulated that the structure of psicose, with all the hydroxyl groups on the same side of the molecule, creates a more favorable environment for binding of the alkali metal cations. From the previous analysis, it is interesting to note that fragments of mass 73 and 91 are small, linear portions of the molecules while fragments of mass 85, 115 and 163 are ring structures. Together, these suggest that the five-membered rings are more stable in the bombardment of primary ions than are the six-membered rings.

This work on underivatized monosaccharides provides a critical first step for analysis of biological samples by ToF-SIMS. We have shown that ToF-SIMS with PCA has sufficient sensitivity to distinguish between closely-related, biologically relevant isomers. Coupled with the reproducibility and sensitivity of the technique, this result will allow discrimination of similar biological samples and elucidation of the ions which are primarily responsible for the spectral differences between samples.

Some potential applications include differentiation of subtle chemical changes in biological samples that may provide insights into cellular processes, disease progress, and disease diagnosis.

Conclusion

This work has demonstrated the application of Time-of-Flight Secondary Ion Mass Spectrometry (ToF-SIMS) coupled to multivariate statistical analysis as a unique analytical method with the necessary reproducibility and selectivity to discriminate between stereoisomers of common monosaccharides. Application of this impressive selectivity will enable routine, small-molecule analysis of complex biological samples. Current research applications of this technology include early detection of cancer, cancer tissue analysis, metabolomics, and investigations into the mechanisms of apoptosis.

ACKNOWLEDGMENT (Word Style “TD_Acknowledgments”). This work was performed under the auspices of the U. S. Department of Energy by the University of California, Lawrence Livermore National Laboratory (LLNL) under Contract No. W-7405-Eng-48. The project 04-ERD-104 was funded by the Laboratory Directed Research and Development Program at LLNL.

REFERENCES (Word Style “TF_References_Section”).

- (1) Belu, A. M.; Graham, D. J.; Castner, D. G. *Biomaterials* **2003**, *24*, 3635-3653.
- (2) Lockyer, N. P.; Vickerman, J. C. *Applied Surface Science* **2004**, *231-232*, 377-384.
- (3) Pachuta, S. J. *Applied Surface Science* **2004**, *231-232*, 217-223.
- (4) Wagner, M. S.; Castner, D. G. *Langmuir* **2001**, *17*, 4649-4660.
- (5) Voet, D.; Voet, J. G. *Biochemistry*, 2 ed.; John Wiley & Sons Inc: New York, New York, 1995.
- (6) Biemann, K.; Schnoes, H. K.; McCloskey, J. A. *Chemistry and Industry* **1963**, 448-449.
- (7) Biemann, K.; DeJongh, D. C.; Schnoes, H. K. *Journal of the American Chemical Society* **1963**, *85*, 1763-1771.
- (8) DeJongh, D. C.; Biemann, K. *Journal of the American Chemical Society* **1963**, *85*, 2289-2294.
- (9) DeJongh, D. C.; Biemann, K. *Journal of the American Chemical Society* **1964**, *86*, 67-74.
- (10) DeJongh, D. C.; Radford, T.; Hribar, J. D.; Hanessian, S.; Bieber, M.; Dawson, G.; Sweeley, C. C. *Journal of the American Chemical Society* **1969**, *91*, 1728-1740.
- (11) Caprioli, R. M.; Seifert, W. E. J. *Biochimica et Biophysica Acta* **1972**, *297*, 213-219.
- (12) Lonngren, J.; Svensson, S. *Advances in Carbohydrate Chemistry and Biochemistry* **1974**, *29*, 42-106.
- (13) Beckey, H. D. *International Journal of Mass Spectrometry and Ion Physics* **1969**, *2*, 500-503.
- (14) Zapfe, S.; Muller, D. *Rapid Communications in Mass Spectrometry* **1998**, *12*, 545-550.
- (15) March, R. E.; Stadey, C. J. *Rapid Communications in Mass Spectrometry* **2005**, *19*, 805-812.

- (16) Taylor, V. F.; March, R. E.; Longerich, H. P.; Stadey, C. J. *International Journal of Mass Spectrometry* **2005**, *243*, 71-84.
- (17) Vink, J.; Bruins Slot, J. H. W.; de Ridder, J. J.; Kamerling, J. P.; Vliegthart, J. F. G. *Journal of the American Chemical Society* **1972**, *94*, 2542-2544.
- (18) Spengler, B.; Dolce, J. W.; Cotter, R. J. *Analytical Chemistry* **1990**, *62*, 1731-1737.
- (19) Hofmeister, G. E.; Zhou, Z.; Leary, J. A. *Journal of the American Chemical Society* **1991**, *113*, 5964-5970.
- (20) Spengler, B.; Kirsch, D.; Kaufmann, R.; Lemoine, J. *Journal of Mass Spectrometry* **1995**, *30*, 782-787.
- (21) Cancilla, M. T.; Wong, A. W.; Voss, L. R.; Lebrilla, C. B. *Analytical Chemistry* **1999**, *71*, 3206-3218.
- (22) Pinheiro, J. C.; Bates, D. M. *Mixed Effects Models in S and S-PLUS*; Springer-Verlag: New York, 2000.
- (23) McLafferty, F. W.; Turecek, F. *Interpretation of Mass Spectra*, 4 ed.; University Science Books: Sausalito, CA, 1993.
- (24) Lemoine, J.; Fournet, B.; Despeyroux, D.; Jennings, K. R.; Rosenberg, R.; de Hoffmann, E. *Journal of the American Society of Mass Spectrometry* **1993**, *4*, 197-203.

SYNOPSIS TOC (Word Style "SN_Synopsis_TOC").

